Magnets are Weber Bar Gravitational Wave Detectors

Valerie Domcke,[1] Sebastian A. R. Ellis,[2] and Nicholas L. Rodd[3,4]
[1]Theoretical Physics Department, CERN, 1 Esplanade des Particules, CH-1211 Geneva 23, Switzerland
[2]Département de Physique Théorique, Université de Genève, 24 quai Ernest Ansermet, 1211 Genève 4, Switzerland
[3]Theory Group, Lawrence Berkeley National Laboratory, Berkeley, California 94720, USA
[4]Berkeley Center for Theoretical Physics, University of California, Berkeley, California 94720, USA

(Received 31 October 2024; revised 17 January 2025; accepted 16 May 2025; published 12 June 2025)

When a gravitational wave (GW) passes through a dc magnetic field, it couples to the conducting wires carrying the currents which generate the magnetic field, causing them to oscillate at the GW frequency. The oscillating currents then generate an ac component through which the GW can be detected—thus forming a resonant mass detector or a *nagnetic Weber bar*. We quantify this claim and demonstrate that magnets can have exceptional sensitivity to GWs over a frequency range demarcated by the mechanical and electromagnetic resonant frequencies of the system; indeed, we outline why a magnetic readout strategy can be considered an optimal Weber bar design. The concept is applicable to a broad class of magnets, but can be particularly well exploited by the powerful magnets being deployed in search of axion dark matter, for example, by DMRadio and ADMX-EFR. Explicitly, we demonstrate that the MRI magnet that is being deployed for ADMX-EFR can achieve a broadband GW strain sensitivity of $\sim 10^{-20}/\sqrt{\mathrm{Hz}}$ from a few kHz to about 10 MHz, with a peak sensitivity down to $\sim 10^{-22}/\sqrt{\mathrm{Hz}}$ at a kHz exploiting a mechanical resonance.

DOI: 10.1103/966v-r5fm

The universality of the gravitational coupling implies there are many ways that a gravitational wave (GW) can interact with matter and therefore many ways GWs could be detected. Nevertheless, the search for GWs has been historically dominated by considering the mechanical coupling of the wave; this underpins the common interpretation of Weber bars [1] and interferometers [2], where the wave couples to a resonant mass or the interferometer mirrors, respectively.

While exploring searches for GWs at higher frequencies ($f > 1$ kHz), the full set of gravitational couplings is being reconsidered, as partially reviewed in Ref. [3]. Two of the leading approaches are to exploit the coupling of GWs to electromagnetism [4–6] or to again rely on the traditional mechanical coupling, but in setups optimized for short wavelength GWs, such as bulk acoustic wave devices [7] or a levitated sensor detector (LSD) [8,9]. An advantage of the mechanical coupling is that the excitations in materials are less stiff than those in electromagnetism—the speed of sound is significantly smaller than the speed of light—making it easier for a GW to mechanically deform or displace objects than to induce an electromagnetic (EM) field. A disadvantage, however, is that the induced mechanical motion then typically needs to be read out by an electromagnetic sensor, involving the need to transduce the mechanical signal to an electromagnetic one.

In this Letter we put forward a proposal that combines the best of these two worlds. We consider the mechanical coupling of a GW to the support structure of a dc magnet, and, in particular, to the conducting wires that generate the magnetic field. Heuristically, the GW leads to an oscillation of the wires with the GW frequency, resulting in a small ac component to the magnetic field. Hence, despite the coupling being mechanical, the generated signal is intrinsically electromagnetic, and can be read out through a SQUID coupled to a pickup loop, with the possibility of enhancing the signal by introducing a resonant LC circuit. Compared to traditional Weber bar detectors, this greatly improves the sensitivity off the mechanical resonance frequency. For a related discussion in the context of resonant cavities, see Ref. [10].

The expected sensitivity of this setup is shown in Fig. 1. The dip around a kHz indicates a mechanical resonance of the magnet with only a single mechanical resonance shown for simplicity. At the resonance the device behaves almost identically to a conventional Weber bar and, remarkably, in this very narrow frequency regime, the achievable strain sensitivity is comparable to that currently achieved by interferometers [11,12] and can surpass the expected broadband sensitivity of the proposed MAGO experiment [10]. The solid projected reach curves assume a broadband

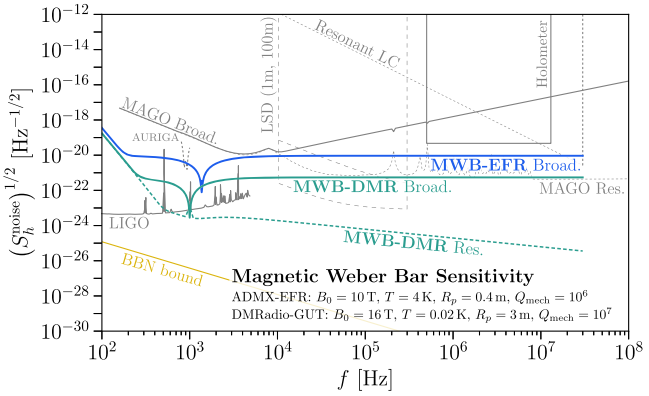

FIG. 1. The noise-equivalent strain power spectral density (PSD) for two different experimental configurations with key parameters given in the legend. The blue line corresponds roughly to the ADMX-EFR magnet [16] with $\ell = 2$ m, while the teal curves correspond roughly to a magnet of the size envisioned for DMRadio-GUT [17] with $\ell = 4$ m. All solid and dashed curves correspond to broadband and resonant readouts, respectively. See text for details.

readout, implying that the achievable signal-to-noise ratio across the entire frequency range benefits from the full instrument integration time. This makes the configuration highly sensitive to transients at unknown frequencies and even for persistent signals as we can exploit their duration. This is in contrast to proposals operating in resonant mode relying on a scanning strategy (dashed gray curves) [6,9,10,13–15], which conventionally optimize their sensitivity over a small frequency range for a short duration before moving on. Supplementing our proposal by coupling to a resonant circuit can improve the strain sensitivity at the corresponding resonant frequency, as we show in dashed teal.

Figure 1 further displays the strain sensitivity corresponding to the cosmological bound on a stochastic gravitational wave background, labelled BBN bound [18]. We emphasize that this comparison depends crucially on how well a given detector is suited to search for stochastic backgrounds. Ground-based interferometers, making use of the cross-correlation across different detectors, currently reach sensitivities about 2 orders of magnitude beyond this limit. More generally, broadband detectors can rely on templates (often simple power laws) for the expected signal spectra to improve the sensitivity by a factor $(t_{\rm int}\Delta f)^{1/4}$, with $t_{\rm int}$ the integration time and Δf the minimum of the signal and analysis bandwidths.

The goal of this Letter is to provide a careful analysis of the claims made so far. We begin, however, with a sketch of the essential idea.

Wiggling a dc magnet—Consider a dc solenoidal magnet of length ℓ made of N coils carrying current I. Unperturbed, it generates a field $B_0 \sim NI/\ell$. Working in the local inertial frame associated with an observer in the laboratory, a passing GW of strain h imparts the equivalent of a Newtonian force on the experiment, slightly deforming its shape. The exact deformation depends on the material properties and geometry of the solenoid. However, if we consider a long thin solenoid and frequencies well above the mechanical resonance, a GW orthogonal to the symmetry axis of the solenoid induces a deformation that is approximately $\ell \to \ell + h\ell$. The solenoid now generates a magnetic field of $B \sim B_0(1-h)$, implying the presence of an ac contribution to the magnetic field oscillating at the GW frequency.

To read out the signal we place a pickup loop of radius R_p through which the GW induces an ac flux of $\Phi \sim hB_0\pi R_p^2$. Imagining a broadband readout, we can estimate our sensitivity by inductively coupling the pickup loop to a SQUID. Taking a characteristic coupling of $\kappa \sim 10^{-2}$ and noise of $\Phi_{\rm SQ} \sim 10^{-21}$ Wb$/\sqrt{\rm Hz}$, the sensitivity expressed as a noise spectral densities is $(S_h^{\rm noise})^{1/2} \sim \Phi_{\rm SQ}/(\kappa B_0 \pi R_p^2) \sim 10^{-20}/\sqrt{\rm Hz}$ for $R_p \sim 0.4$ m and $B_0 \sim 10$ T, consistent with Fig. 1. For a persistent monochromatic GW signal, the strain sensitivity of a ten day observation would be $h \sim (S_h^{\rm noise}/T)^{1/2} \sim 10^{-23}$, which could probe GWs emitted by axion superradiance at around 0.1 MHz, an idea which has been broadly explored, see, e.g., Refs. [8,9,19–31]. We validate the accuracy of these heuristic estimates of the signal and noise in the following sections.

Before doing so, let us briefly justify where our concept improves over existing approaches. Comparing with traditional Weber bars, the main advantage lies in inherently large EM energy in a magnetic readout, enabling an efficient measurement of the mechanical deformation. Comparing to a direct coupling of the GW to the EM field, we profit from the reduced stiffness of the mechanical deformations at frequencies below the EM resonance. Both comparisons are discussed in greater detail in the Supplemental Material [32], which includes Refs. [33–41].

Induced magnetic field—Throughout this Letter we work in the proper detector frame, in which the GW acts by exerting a Newtonian force

$$F_i^h/m = \frac{1}{2}\ddot{h}_{ij}^{\rm TT}\boldsymbol{r}^j, \tag{1}$$

acting on a test particle of mass m at position $\boldsymbol{r}$, with $h_{ij}^{\rm TT}$ indicating the GW tensor evaluated in the transverse traceless frame, which depends on the amplitude for the two polarizations h_+ and $h_\times$. Explicitly, we decompose a GW propagating along the x axis as $h_{ij}^{\rm TT}(t) = h_A e_{ij}^A e^{-i\omega(t-x)}$, where $A = +, \times$, and e_{ij}^A are the polarization tensors, with explicit forms given in Supplemental Material [32]. We consider the impact of this force on a solenoidal magnetic field, generated by a current-carrying spool. In detail, the force will perturb both the position and orientation of the spool through which the currents are running. As we show in

Supplemental Material [32], applying the Biot-Savart law yields

$$\mathbf{B}(\boldsymbol{r}') = \int_V d^3\boldsymbol{r}\frac{\boldsymbol{j}(\boldsymbol{r})\times[\boldsymbol{r}'-\boldsymbol{\xi}(\boldsymbol{r})]}{4\pi|\boldsymbol{r}'-\boldsymbol{\xi}(\boldsymbol{r})|^3}. \tag{2}$$

The volume integral is performed over the unperturbed (flat space) coordinates of the spool. The deformation of the spool's location by the GW is encoded in $\boldsymbol{\xi}(\boldsymbol{r}) = \boldsymbol{r} + \boldsymbol{\delta r}(\boldsymbol{r})$ and we discuss how this is determined shortly. Henceforth we leave the dependence on $\boldsymbol{r}$ implicit. The current density is given by

$$\boldsymbol{j} = \frac{I_N}{\ell\,\Delta r}\frac{d\boldsymbol{\xi}}{d\phi}\left|\frac{d\boldsymbol{\xi}}{d\phi}\right|^{-1}, \tag{3}$$

with $I_N = NI$ denoting the ampere turns of the current, Δr the radial width of the spool, ℓ its length, and the remaining factors indicating the orientation of the current in the presence of a GW.

Equation (2) demonstrates that the GW modifies the magnetic field generated by the spool, adding an oscillatory component at the GW frequency. We can read this out with a pickup loop that is sensitive to the field at all positions $\boldsymbol{r}'$ within its area. In computing this effect, one must account for the fact the pickup loop itself is subject to the GW force. In the following, we will assume the pickup loop to be suspended, so that we can treat its motion as approximately free-falling, i.e., the GW perturbs the flat space position $\boldsymbol{r}'_0$ to $\boldsymbol{r}' = \boldsymbol{r}'_0 + \boldsymbol{\delta r}'_{\rm ff}$. We do not consider possible mechanical resonances of the pickup loop, as with the geometry envisioned, the dominant effect is well captured in this approximation. In that limit, the deformation of the pickup loop is simply given by the Newtonian force of Eq. (1),

$$\ddot{\boldsymbol{\delta r}}'_{{\rm ff},i} = \frac{1}{2}\ddot{h}^{\rm TT}_{ij}\boldsymbol{r}'^{j}_0. \tag{4}$$

We note that the above treatment cannot be extended to arbitrarily low frequencies. Once the GW frequency falls below the restoring frequency of the suspensions system employed for the pickup loop, the magnet and loop would begin to move in concert, suppressing our sensitivity.

What remains is to determine the deformation of the spool $\boldsymbol{\delta r}$. We consider two approaches. Well above the resonant frequencies of the spool, the GW acts as a driving frequency the material cannot respond to in time, implying we can take the free-falling limit with $\boldsymbol{\delta r}$ determined from Eq. (4). This corresponds to the molecules of the spool material responding individually to the GW. At lower frequencies, we must account for the response of the material to the imposed force. We do so using the mechanical eigenmodes of the magnet parametrized by dimensionless displacements $\boldsymbol{u}_{mnp}(\boldsymbol{r})$, with (m, n, p) labeling the order of the modes in the polar, radial, and longitudinal directions. Details of how these modes can be approximated for a finite width cylinder are provided in Supplemental Material [32]. The mechanical response of the magnet to an incoming GW is parametrized in terms of dimensionless overlap factors,

$$\eta^A_{mnp} = \frac{1}{2V\ell_\eta}\int_V d^3\boldsymbol{r}\, e^A_{ij}\boldsymbol{r}^i[\boldsymbol{u}^*_{mnp}]^j, \tag{5}$$

normalized such that if we sent $[\boldsymbol{u}^*_{mnp}]^j \to \frac{1}{2}e^A_{ij}\boldsymbol{r}^j/\ell_\eta$ for either polarization we obtain $\eta = 1$. As an example to demonstrate that $\mathcal{O}(1)$ couplings are possible, consider a mode that we expect to strongly couple to a GW traveling along the z axis, $\boldsymbol{u}_{210}$ (the explicit form is given in Supplemental Material [32]). If we take a spool of length 2 m and inner and outer radii of 0.6 and 0.65 m, we find a coupling of $\eta^{+,\times}_{210} \simeq 0.95$, with the $+(\times)$ polarization of the GW coupling to the 210 mode with odd (even) azimuthal dependence. A GW incident along the x axis will also couple to this mode, albeit with a reduced coupling of $\eta^{+}_{210} \simeq 0.41$ and $\eta^{\times}_{210} \simeq 0$. The magnet dimensions are inspired by the MRI magnet to be used for ADMX-EFR, which has a peak magnetic field of $B_0 \simeq 10$ T generated by a current of ~20 MA-turns. The eigenfrequency of this mode is determined by the diameter of the spool, and for the dimensions above is found to be at $f \simeq 1.4$ kHz for a stainless steel cylinder. To compute the induced magnetic field we insert $\boldsymbol{\delta r} = \eta_{210}\boldsymbol{u}_{210}\ell_\eta$ into $\boldsymbol{\xi}$, which can be enhanced by the mechanical quality factor $Q_{\rm mech}$ on resonance, in Eq. (2) and otherwise proceed as in the freely falling limit.

The precise magnitude of the signal depends on the position and orientation of the pickup loop, and we provide numerical results for different frequency regimes in Supplemental Material [32]. For example, one can obtain a large signal by placing a pickup loop close to an end cap of the magnet, where the external magnetic field is still rather strong but features a significant gradient. With a suitable placement of the pickup loop, we expect induced magnetic fields of $\mathcal{O}(hB_0)$ at frequencies away from the mechanical resonance and $\mathcal{O}(hQ_{\rm mech}B_0)$ on the mechanical resonance. In a realistic setup, material simulations and measurements will be needed to determine the precise mechanical response of the system.

Signal-to-noise ratio (SNR)—The optimal SNR for the strain h can be written as (As written, this SNR is quadratic in h. For a signal whose waveform can be matched in the time domain, an SNR that is linear in strain can be constructed by performing a matched filtering analysis. Doing so leads to an SNR that is identical to Eq. (6), only with the frequency integral taken over the ratio of unsquared PSDs.)

$$\mathrm{SNR}^2 \simeq 2t_{\mathrm{int}} \int_0^\infty df \left(\frac{S_{\mathrm{sig}}(f)}{S_{\mathrm{noise}}(f)}\right)^2. \quad (6)$$

As derived explicitly in Supplemental Material [32], the signal power spectral density (PSD) enters in the form of a PSD of the flux through the pickup loop. Explicitly, $S_{\mathrm{sig}}(f) = B_0^2 A_p^2 |\mathcal{G}(f,\boldsymbol{x})|^2 S_h(f)$, where A_p is the pickup loop area, $S_h(f)$ is the GW PSD, whil $\mathcal{G}(f,\boldsymbol{x})$ is a dimensionless gain factor that depends on the GW frequency as well as the position and orientation of the pickup loop and which must be computed numerically. Lastly, $S_{\mathrm{noise}}(f)$ represents the PSD of various noise sources that we enumerate in Supplemental Material [32].

The dimensionless gain factor arises from the two contributions to the magnetic flux that traverses the pickup loop, as discussed in the previous section. The first is the coupling of the GW to the spool. Numerically, we conservatively only include the gain generated from the GW coupling to the 210 mode as discussed above; in principle, there are contributions from all modes to which the GW couples, although this mode will dominate for a GW propagating along the z direction. The second contribution comes from the relative motion of the freely falling pickup loop with respect to the magnet.

Let us consider the expected behavior of the gain in three limits around the lowest-lying mechanical resonance of the spool f_{min}: 1. $f \ll f_{\mathrm{min}}$; 2. $f \sim f_{\mathrm{min}}$; and 3. $f \gg f_{\mathrm{min}}$. In the first case, the low frequency limit, the mechanical coupling to the spool is suppressed by $(f/f_{\mathrm{min}})^2$, whereas the coupling to the freely falling pickup loop is not. Consequently, the latter dominates, leaving $|\mathcal{G}|^2_{f\ll f_{\mathrm{min}}} \lesssim 1$. In this regime, the SQUID noise is likely to dominate in a broadband setup. As a result, if both the signal and noise PSDs can be approximated as flat in a bandwidth Δf, the SNR for this regime can be obtained from Eq. (6) as

$$\mathrm{SNR}_{\mathrm{f}\ll\mathrm{f}_{\mathrm{min}}} \sim (t_{\mathrm{int}}\Delta f)^{1/2} \frac{S_h(f) B_0^2 A_p^2}{S^{\mathrm{SQ}}_{\mathrm{noise}}(f)}. \quad (7)$$

In the second regime, where the GW frequency matches a mechanical resonance $f \sim f_{\mathrm{min}}$, the gain is dominated by the mechanical quality factor moderating the response of that mode. The gain again depends on the positioning of the pickup loop (see Supplemental Material [32]), although largest it can be is $|\mathcal{G}|^2 \sim Q^2_{\mathrm{mech}}$. In this case, thermal mechanical noise in the magnet dominates for typical parameter choices, in which case one would not gain further with a resonant rather than broadband EM readout (as seen in Fig. 1). (We note that thermal noise in the pickup loop remains subdominant at all frequencies.) The resulting SNR scales as

$$\mathrm{SNR}_{\mathrm{mech\ res}} \sim (t_{\mathrm{int}}\Delta f)^{1/2} \frac{Q_{\mathrm{mech}} S_h(f) \ell_h^2 M \omega^3_{\mathrm{mech}}}{2T}, \quad (8)$$

where M is the mass of the magnet, T its temperature, and the characteristic scale of the deformations induced by the GW is $\ell_h = \eta \ell_\eta$, written in terms of the overlap factor in Eq. (5). (The reader should be cautioned that taking the $M \to \infty$ limit does not infinitely improve the SNR. For a broadband readout, eventually SQUID noise again becomes the dominant background and the SNR saturates at $Q^2_{\mathrm{mech}} \times \mathrm{SNR}_{\mathrm{f}\ll\mathrm{f}_{\mathrm{min}}}$.) In this thermally limited mechanically resonant scenario, the broadband SNR scales as Q_{mech} owing to the suppression of the thermal mechanical noise by the mechanical resonance's linewidth, $\omega_{\mathrm{mech}}/Q_{\mathrm{mech}}$.

Last, we turn to the limit where $f \gg f_{\mathrm{min}}$. Now we are in the flexible regime discussed previously, and the gain is approximately $|\mathcal{G}|^2 \lesssim 1$. In this regime, the $\boldsymbol{u}_{210}$ mode responds flexibly, and the sum over all modes would approximate the free-falling magnet limit. SQUID noise is expected to dominate, and the SNR is again approximated by Eq. (7).

In all three regimes discussed above, we have assumed that the pickup loop is placed just outside the magnet. Flux conservation through the superconducting magnet coils implies that for $f \gg f_{\mathrm{min}}$ there will be no signal through a coaxial loop placed inside the magnet.

Note that the noise sources we consider here will dominate as long as there is sufficient shielding against ambient magnetic field noise. Given the anticipated magnetic field noise of $B(f) \lesssim 10^{-14}\ \mathrm{T}/\sqrt{\mathrm{Hz}}$ at frequencies $f \gtrsim 100$ Hz [42], the shielding requires a reduction of at most 10^7 in the field amplitude. This could be achieved, for example, with a 5 mm-thick iron-nickel alloy shield with $\mu_r = 75 \times 10^3, \sigma = 2 \times 10^6\ \mathrm{S/m}$ [43].

Sensitivity—The expressions from the previous section can be used to determine the sensitivity of a single detector to both stochastic GW sources, where the bin width Δf depends on the expected spectral shape of the GW signal, and to coherent sources for which one should take $S_h(f) \sim h_0^2/\Delta f$. The information can also be used to determine the expected sensitivity of the detector as encoded in the noise-equivalent strain, which is shown in Fig. 1. Formally, the noise-equivalent strain PSD is defined as $S_h^{\mathrm{noise}}(f) \equiv S_{\mathrm{noise}}(f) S_h(f)/S_{\mathrm{sig}}(f)$. Detailed expressions for each component are provided in Supplemental Material [32].

We can already estimate the form of $S_h^{\mathrm{noise}}(f)$ from the details of the previous section. In particular, taking the form for the signal PSD discussed below Eq. (6), we have $S_h^{\mathrm{noise}}(f) \sim S_{\mathrm{noise}}(f)/B_0^2 A_p^2 |\mathcal{G}(f,\boldsymbol{x})|^2$, exposing its various dependencies. In Fig. 1 we assume a gain of $|\mathcal{G}|^2 = 5$ away from a mechanical resonance, whereas on the resonance we directly compute the sensitivity by comparing the displacement PSDs as detailed in Supplemental Material [32]. Combining these two approaches we find a slight degradation in the sensitivity at the mechanical resonance. These

specific sensitivities correspond to the values found for the single mode studied in Supplemental Material [32], so it is likely that a detailed numerical study including all modes and optimising the loop placement can improve upon these. In particular, we anticipate the possibility of improvement around a mechanical resonance of a mode with a longitudinal component. Of course, the additional modes would also enhance the thermal noise at their respective locations, which we have neglected in our projections.

Finally, coupling the pickup loop to an LC circuit with EM quality factor $Q_{\rm EM}$ can improve the sensitivity in parts of the parameter space at the cost of reducing the detector bandwidth. As a simple estimate, on the mechanical resonance the SNR would remain the same as in the broadband case of Eq. (8) (and therefore again the sensitivity slightly degrades), whereas above the mechanical resonance, the SNR would improve from Eq. (7) by a factor $\sim 10^5 \times (f/10^4\ \text{Hz})$ assuming resonant LC circuit parameters of $T_{\rm LC} = 10$ mK and $Q_{\rm EM} = 2 \times 10^7$, comparable to DMRadio-GUT [17]. The intrinsic bandwidth of the LC resonator $\Delta f_{\rm LC}$ can affect the determination of Δf in the resulting expressions for the SNR. For more details, see Supplemental Material [32].

In Fig. 1, we have taken two hypothetical magnet and pickup loop configurations, inspired by the ADMX-EFR and DMRadio-GUT magnets. The main parameters we have chosen for both are described in the figure caption. For the ADMX-EFR-inspired scenario, we computed the resonant frequency of the u_{210} mode, and assumed it has a quality factor of $Q_{\rm mech} = 10^6$. For the DMRadio-GUT-inspired configuration, we assume $Q_{\rm mech} = 10^7$ and a resonance at $f_{\rm min} = 1$ kHz, justified by the large magnet dimensions. For ADMX-EFR we assumed a similar magnet temperature as achieved for AURIGA of 4 K, whereas for DMRadio-GUT we adopted a more aggressive 0.02 K, although this only impacts the sensitivity on the mechanical resonance. We conservatively assume that both magnets weigh $M = 40$ tons (similar to previous resonant mass experiments [44]), such that any increase in the DMRadio-GUT magnet mass could be absorbed by an overestimate in the mechanical quality factor. For simplicity we assume persistent superconducting magnets, otherwise additional noise associated with the external power supply must be included. Two pickup loop configurations were employed: A co-axial loop (off-resonance sensitivity) and a quarter-circle loop (sensitivity on resonance), both placed close to the endcap of the magnet. The sensitivity further assumes seismic isolation of the apparatus through a dual suspension system assuming a quiet site [45], which is eventually overcome leading to a loss in sensitivity at low frequencies. Even in the case of full seismic isolation, the suspension system is likely to contribute to a deterioration of the sensitivity below $f \lesssim 100$ Hz, a frequency associated to the typical size of an experimental hall, and eventually gravity gradient noise [46,47] will become relevant.

Conclusions—The focus of this Letter has been to demonstrate that dc magnets can act as remarkably sensitive GW detectors. The mechanical force exerted by a GW on the magnet itself and on a pickup loop placed within the magnetic field directly induces an ac magnetic flux component through the pickup loop. Our estimate for the resulting sensitivity is shown in Fig. 1; our projected noise-equivalent strain with a broadband readout is stronger than many projections achieve with a narrow band resonant readout. Our more conservative estimate is based on the magnet dimensions suggested for ADMX-EFR [16], and can be easily generalized to other powerful magnets, such as the GrAHal magnet [48] or the magnets envisioned for DMRadio [17,49,50]. Away from the mechanical resonance, our sensitivity could also be improved with the use of a resonant EM readout.

Looking forward, the observations of this Letter will impact GW searches relying on static magnetic fields. The most obvious connection is to searches inspired by low-mass axion haloscopes [6]. For toroidal magnets (as used for ABRA-10 cm [51–53] or SHAFT [54]) the effect discussed here is irrelevant as the pickup loop is typically placed in a field free region. On the contrary, for solenoidal magnets (as used in BASE [55], WISPLC [56], ADMX SLIC [57], and proposed for DMRadio-m^3 [49,50]), both the contribution discussed here and the contribution from the EM coupling [58] are present. The details depend on the placement of the pickup loop, but as discussed, we expect the mechanical signal to dominate below the EM resonant frequency. As a general statement, our work is an explicit realization of the fact that in the presence of a GW, any laboratory magnetic field cannot be considered static. This is particularly relevant at frequencies around the mechanical resonances, where the magnet can be treated neither as rigid (low frequency limit) or as free falling (high frequency limit), see also Ref. [59].

Acknowledgments—We thank Krisztian Peters and Jérémie Quevillon for helpful feedback. We particularly thank Aaron Chou for helpful feedback regarding flux conservation through a superconducting wire, and Andrew Sonnenschein for discussions and providing details regarding the ADMX-EFR magnet. We further thank Kaliroë Pappas and Jan Schütte-Engel for useful comments on a draft version of this work. The work of S. A. R. E. was supported by SNF Ambizione Grant No. PZ00P2_193322, *New frontiers from sub-eV to super-TeV*. The work of N. L. R. was supported by the Office of High Energy Physics of the U.S. Department of Energy under Contract No. DE-AC02-05CH11231. Part of this work was performed at Aspen Center for Physics, which is supported by National Science Foundation Grant No. PHY-2210452.

[1] J. Weber, Gravitational radiation, Phys. Rev. Lett. **18**, 498 (1967).

[2] M. E. Gertsenshtein and V. I. Pustovoit, On the detection of low frequency gravitational waves, Sov. Phys. JETP **16**, 433 (1962), https://ui.adsabs.harvard.edu/abs/1963JETP...16..433G/abstract.

[3] N. Aggarwal *et al.*, Challenges and opportunities of gravitational-wave searches at MHz to GHz frequencies, Living Rev. Relativity **24**, 4 (2021).

[4] A. Ejlli, D. Ejlli, A. M. Cruise, G. Pisano, and H. Grote, Upper limits on the amplitude of ultra-high-frequency gravitational waves from graviton to photon conversion, Eur. Phys. J. C **79**, 1032 (2019).

[5] A. Berlin, D. Blas, R. Tito D'Agnolo, S. A. R. Ellis, R. Harnik, Y. Kahn, and J. Schütte-Engel, Detecting high-frequency gravitational waves with microwave cavities, Phys. Rev. D **105**, 116011 (2022).

[6] V. Domcke, C. Garcia-Cely, and N. L. Rodd, Novel search for high-frequency gravitational waves with low-mass axion haloscopes, Phys. Rev. Lett. **129**, 041101 (2022).

[7] M. Goryachev and M. E. Tobar, Gravitational wave detection with high frequency phonon trapping acoustic cavities, Phys. Rev. D **90**, 102005 (2014).

[8] A. Arvanitaki and A. A. Geraci, Detecting high-frequency gravitational waves with optically-levitated sensors, Phys. Rev. Lett. **110**, 071105 (2013).

[9] N. Aggarwal, G. P. Winstone, M. Teo, M. Baryakhtar, S. L. Larson, V. Kalogera, and A. A. Geraci, Searching for new physics with a levitated-sensor-based gravitational-wave detector, Phys. Rev. Lett. **128**, 111101 (2022).

[10] A. Berlin, D. Blas, R. Tito D'Agnolo, S. A. R. Ellis, R. Harnik, Y. Kahn, J. Schütte-Engel, and M. Wentzel, Electromagnetic cavities as mechanical bars for gravitational waves, Phys. Rev. D **108**, 084058 (2023).

[11] A. Buikema *et al.*, Sensitivity and performance of the Advanced LIGO detectors in the third observing run, Phys. Rev. D **102**, 062003 (2020).

[12] A. S. Chou *et al.* (Holometer Collaboration), MHz gravitational wave constraints with decameter Michelson interferometers, Phys. Rev. D **95**, 063002 (2017).

[13] A. Vinante (AURIGA Collaboration), Present performance and future upgrades of the AURIGA capacitive readout, Classical Quantum Gravity **23**, S103 (2006).

[14] M. Cerdonio *et al.*, The ultracryogenic gravitational wave detector AURIGA, Classical Quantum Gravity **14**, 1491 (1997).

[15] M. Goryachev, W. M. Campbell, I. S. Heng, S. Galliou, E. N. Ivanov, and M. E. Tobar, Rare events detected with a bulk acoustic wave high frequency gravitational wave antenna, Phys. Rev. Lett. **127**, 071102 (2021).

[16] S. Knirck (ADMX Collaboration Team), ADMX extended frequency range (EFR): Searching for 2–4 GHz axions with 18 cavities, in *APS April Meeting Abstracts*, Vol. 2023 of APS Meeting Abstracts (2023), p. CCC01.002.

[17] L. Brouwer *et al.* (DMRadio Collaboration), Proposal for a definitive search for GUT-scale QCD axions, Phys. Rev. D **106**, 112003 (2022).

[18] T.-H. Yeh, J. Shelton, K. A. Olive, and B. D. Fields, Probing physics beyond the standard model: Limits from BBN and the CMB independently and combined, J. Cosmol. Astropart. Phys. 10 (2022) 046.

[19] I. M. Ternov, V. R. Khalilov, G. A. Chizhov, and A. B. Gaina, Finite motion of massive particles in the Kerr and Schwarzschild fields, Sov. Phys. J. **21**, 1200 (1978).

[20] T. J. M. Zouros and D. M. Eardley, Instabilities of massive scalar perturbations of a rotating black hole, Ann. Phys. (N.Y.) **118**, 139 (1979).

[21] S. L. Detweiler, Klein-Gordon equation and rotating black holes, Phys. Rev. D **22**, 2323 (1980).

[22] A. Arvanitaki, S. Dimopoulos, S. Dubovsky, N. Kaloper, and J. March-Russell, String axiverse, Phys. Rev. D **81**, 123530 (2010).

[23] A. Arvanitaki and S. Dubovsky, Exploring the string axiverse with precision black hole physics, Phys. Rev. D **83**, 044026 (2011).

[24] H. Yoshino and H. Kodama, Gravitational radiation from an axion cloud around a black hole: Superradiant phase, Prog. Theor. Exp. Phys. **2014**, 043E02 (2014).

[25] R. Brito, V. Cardoso, and P. Pani, Black holes as particle detectors: Evolution of superradiant instabilities, Classical Quantum Gravity **32**, 134001 (2015).

[26] A. Arvanitaki, M. Baryakhtar, and X. Huang, Discovering the QCD axion with black holes and gravitational waves, Phys. Rev. D **91**, 084011 (2015).

[27] R. Brito, V. Cardoso, and P. Pani, Superradiance: New frontiers in black hole physics, Lect. Notes Phys. **906**, 1 (2015).

[28] R. Brito, S. Ghosh, E. Barausse, E. Berti, V. Cardoso, I. Dvorkin, A. Klein, and P. Pani, Gravitational wave searches for ultralight bosons with LIGO and LISA, Phys. Rev. D **96**, 064050 (2017).

[29] L. Tsukada, T. Callister, A. Matas, and P. Meyers, First search for a stochastic gravitational-wave background from ultralight bosons, Phys. Rev. D **99**, 103015 (2019).

[30] S. J. Zhu, M. Baryakhtar, M. A. Papa, D. Tsuna, N. Kawanaka, and H.-B. Eggenstein, Characterizing the continuous gravitational-wave signal from boson clouds around Galactic isolated black holes, Phys. Rev. D **102**, 063020 (2020).

[31] D. Brzeminski, A. Hook, J. Huang, and C. Ristow, Searching for string bosenovas with gravitational wave detectors, J. High Energy Phys. 01 (2025) 007.

[32] See Supplemental Material at http://link.aps.org/supplemental/10.1103/966v-r5fm for details.

[33] Y. Kahn, B. R. Safdi, and J. Thaler, Broadband and resonant approaches to axion dark matter detection, Phys. Rev. Lett. **117**, 141801 (2016).

[34] M. Bonaldi, M. Cerdonio, L. Conti, M. Pinard, G. A. Prodi, and J. P. Zendri, Selective readout and back action reduction for wideband acoustic gravitational wave detectors, Phys. Rev. D **68**, 102004 (2003).

[35] S. Sendelbach, D. Hover, A. Kittel, M. Mück, J. M. Martinis, and R. McDermott, Magnetism in squids at millikelvin temperatures, Phys. Rev. Lett. **100**, 227006 (2008).

[36] P. Kumar, S. Sendelbach, M. A. Beck, J. W. Freeland, Z. Wang, H. Wang, C. C. Yu, R. Q. Wu, D. P. Pappas, and R. McDermott, Origin and reduction of $1/f$ magnetic flux noise in superconducting devices, Phys. Rev. Appl. **6**, 041001 (2016).

[37] D. A. Rower, L. Ateshian, L. H. Li, M. Hays, D. Bluvstein, L. Ding, B. Kannan, A. Almanakly, J. Braumüller, D. K. Kim *et al.*, Evolution of $1/f$ flux noise in superconducting

qubits with weak magnetic fields, Phys. Rev. Lett. **130**, 220602 (2023).
[38] R. Kubo, The fluctuation-dissipation theorem, Rep. Prog. Phys. **29**, 255 (1966).
[39] P. R. Saulson, Thermal noise in mechanical experiments, Phys. Rev. D **42**, 2437 (1990).
[40] J. W. Foster, N. L. Rodd, and B. R. Safdi, Revealing the dark matter halo with axion direct detection, Phys. Rev. D **97**, 123006 (2018).
[41] J. N. Benabou, J. W. Foster, Y. Kahn, B. R. Safdi, and C. P. Salemi, Lumped-element axion dark matter detection beyond the magnetoquasistatic limit, Phys. Rev. D **108**, 035009 (2023).
[42] C. Constable and S. Constable, A grand spectrum of the geomagnetic field, Phys. Earth Planet. Inter. **344**, 107090 (2023).
[43] S. Celozzi, R. Araneo, P. Burghignoli, and G. Lovat, *Electromagnetic Shielding: Theory and Applications* (John Wiley & Sons, New York, 2023).
[44] L. Gottardi, Complete model of a spherical gravitational wave detector with capacitive transducers: Calibration and sensitivity optimization, Phys. Rev. D **75**, 022002 (2007).
[45] P. R. Saulson, *Fundamentals of Interferometric Gravitational Wave Detectors*, 2nd ed. (World Scientific, Singapore, 2017).
[46] P. R. Saulson, Terrestrial gravitational noise on a gravitational wave antenna, Phys. Rev. D **30**, 732 (1984).
[47] S. A. Hughes and K. S. Thorne, Seismic gravity gradient noise in interferometric gravitational wave detectors, Phys. Rev. D **58**, 122002 (1998).
[48] T. Grenet, R. Ballou, Q. Basto, K. Martineau, P. Perrier, P. Pugnat, J. Quevillon, N. Roch, and C. Smith, The grenoble axion haloscope platform (GrAHal): Development plan and first results, arXiv:2110.14406.
[49] L. Brouwer *et al.* (DMRadio Collaboration), Projected sensitivity of DMRadio-m3: A search for the QCD axion below 1 μeV, Phys. Rev. D **106**, 103008 (2022).
[50] A. AlShirawi *et al.* (DMRadio Collaboration), Electromagnetic modeling and science reach of DMRadio-m^3, arXiv:2302.14084.
[51] J. L. Ouellet *et al.*, First results from ABRACADABRA-10 cm: A search for sub-μeV axion dark matter, Phys. Rev. Lett. **122**, 121802 (2019).
[52] J. L. Ouellet *et al.*, Design and implementation of the ABRACADABRA-10 cm axion dark matter search, Phys. Rev. D **99**, 052012 (2019).
[53] C. P. Salemi *et al.*, Search for low-mass axion dark matter with ABRACADABRA-10 cm, Phys. Rev. Lett. **127**, 081801 (2021).
[54] A. V. Gramolin, D. Aybas, D. Johnson, J. Adam, and A. O. Sushkov, Search for axion-like dark matter with ferromagnets, Nat. Phys. **17**, 79 (2021).
[55] J. A. Devlin *et al.*, Constraints on the coupling between axionlike dark matter and photons using an antiproton superconducting tuned detection circuit in a cryogenic penning trap, Phys. Rev. Lett. **126**, 041301 (2021).
[56] Z. Zhang, D. Horns, and O. Ghosh, Search for dark matter with an LC circuit, Phys. Rev. D **106**, 023003 (2022).
[57] N. Crisosto, P. Sikivie, N. S. Sullivan, D. B. Tanner, J. Yang, and G. Rybka, ADMX SLIC: Results from a superconducting *LC* circuit investigating cold axions, Phys. Rev. Lett. **124**, 241101 (2020).
[58] V. Domcke, C. Garcia-Cely, S. M. Lee, and N. L. Rodd, Symmetries and selection rules: Optimising axion haloscopes for gravitational wave searches, J. High Energy Phys. 03 (2024) 128.
[59] W. Ratzinger, S. Schenk, and P. Schwaller, A coordinate-independent formalism for detecting high-frequency gravitational waves, J. High Energy Phys. 08 (2024) 195.